Published in final edited form as:
*J Pharm Sci*. 2014 March ; 103(3): 796–809. doi:10.1002/jps.23839.

# Structural Characterization of IgG1 mAb Aggregates and Particles Generated under Various Stress Conditions

**Srivalli N. Telikepalli**[1], **Ozan S. Kumru**[1], **Cavan Kalonia**[1], **Reza Esfandiary**[1,2], **Sangeeta B. Joshi**[1], **C. Russell Middaugh**[1], and **David B. Volkin**[1,*]

[1]Department of Pharmaceutical Chemistry, Macromolecule and Vaccine Stabilization Center, University of Kansas, Lawrence, KS 66047

## Abstract

IgG1 mAb solutions were prepared with and without sodium chloride and subjected to different environmental stresses. Formation of aggregates and particles of varying size was monitored by a combination of size exclusion chromatography (SEC), Nanosight Tracking Analysis (NTA), Micro-flow Imaging (MFI), turbidity, and visual assessments. Stirring and heating induced the highest concentration of particles. In general, the presence of NaCl enhanced this effect. The morphology of the particles formed from mAb samples exposed to different stresses was analyzed from TEM and MFI images. Shaking samples without NaCl generated the most fibrillar particles, while stirring created largely spherical particles. The composition of the particles was evaluated for covalent cross-linking by SDS-PAGE, overall secondary structure by FTIR microscopy, and surface apolarity by extrinsic fluorescence spectroscopy. Freeze-thaw and shaking led to particles containing protein with native-like secondary structure. Heating and stirring produced IgG1 containing aggregates and particles with some non-native disulfide crosslinks, varying levels of intermolecular beta sheet content, and increased surface hydrophobicity. These results highlight the importance of evaluating protein particle morphology and composition, in addition to particle number and size distributions, to better understand the effect of solution conditions and environmental stresses on the formation of protein particles in mAb solutions.

### Keywords

protein; aggregation; particles; formulation; monoclonal antibody; IgG; accelerated stability

## INTRODUCTION

A current concern with the use of monoclonal antibody-based therapeutics is their tendency to aggregate and form particles during long-term storage and/or during accidental exposure to environmental stresses. The formation of aggregates and particles may lead to an increase

[*]Corresponding author: D.B. Volkin, Multidisciplinary Research Building, 2030 Becker Dr., Lawrence, KS 66047. Phone: (785) 864-6262; volkin@ku.edu.
[2]Current address: Department of Formulation Sciences, MedImmune, Gaithersburg, MD 20878

**SUPPORTING INFORMATION AVAILABLE**

This article contains supplementary material available from the authors upon request or via the Internet at http://onlinelibrary.wiley.com.

in immune response [1-3] or a decrease in efficacy of the drug.[2,4] Protein aggregation can occur during many stages of production (purification, formulation, and filling), or during long-term storage, shipping, and even administration to the patient.[5] Therefore it is important to better understand the reasons for aggregation and particle formation due to different stresses and formulation conditions in order to develop strategies to minimize its occurrence.

Aggregation and particle formation in therapeutic protein formulations can be caused by a variety of environmental stresses or by formulation conditions such as concentration,[6-8] solution pH,[6,9,10] and the presence or absence of certain excipients.[6,7,9] Freezing can not only lead to changes in the formulation pH[6,11,12] and concentration of proteins and excipients,[6] but also to the formation of ice/water interfaces[6,13-15] where protein adsorption can induce partial protein unfolding and subsequent aggregation.[6,9,15-17] Proteins subjected to heating undergo conformational changes that can lead to the formation of aggregates and particles.[9,18] Mechanical stresses may cause shear or interfacial effects in which the protein adsorbs to the air-water interface, leading to structural alterations which can initiate aggregation as well.[9,16,19,20] Stirring and shaking are both mechanical stresses that can also cause cavitation, local thermal effects, bubble entrapment, and transportation of the aggregated protein from the air-water or air-container interface into the bulk solution.[6,21,2223]

One major challenge in studying protein aggregation experimentally is that a wide variety of analytical techniques are required to characterize the formation of protein aggregates and particles over a broad size range (from few nanometer to hundreds of microns).[24] In addition, it is also important to have complimentary, orthogonal techniques for analyzing aggregates of similar size ranges since results can differ based on the principles and setup of each technique.[6] In this work, we follow the previously proposed definitions of protein aggregates, across the size ranges of few nanometers to 100s of microns. [25] In this case study, size exclusion chromatography (SEC) is used to analyze smaller aggregates in the size range of tens of nanometers. Although it is a powerful analytical tool for monitoring small nanometer-sized soluble aggregates, upon injection of sample into the column, aggregates can potentially dissociate upon mixing with mobile phase or adhere to the column thereby requiring careful method development and use of orthogonal techniques.[26] For sizing submicron particles (0.1 to 1 μm), Nanosight Tracking Analysis (NTA) is used while for micron (1-100 μm) size particles, Microflow-Imaging technique (MFI) is employed. NTA tracks and sizes individual particles (unlike its DLS counterpart), but has limited sensitivity in detecting low numbers of submicron particles. In addition to sizing and counting particles like light obscuration, MFI also has digital imaging capabilities that can provide morphological information allowing differentiation between silicone and protein particles. To detect visible particles larger than 100 μm, visual assessments are employed. Turbidity is also used as a general method to monitor the formation of aggregates and particles in solution across the various size ranges. Although visual inspection is a commonly used technique, even under pre-defined conditions and with extensive analyst training, results may vary between different analysts. Turbidity provides semi-quantitative information for comparisons of the overall aggregation state of a sample, but it does not provide information regarding the size or number of particles. Detailed discussions of the

strengths and limitations of these analytical techniques are described more thoroughly elsewhere.[27,28]

Recently, there has been an increased emphasis on characterizing the morphology and composition of particles in addition to counting and sizing them.[27] As a starting point for this work, MFI analysis, in addition to sizing and counting of subvisible particles, is used for morphological analysis by utilizing parameters such as aspect ratio and intensity of the digital images.[29,30] For visualization of small, nanometer-sized aggregates, transmission electron microscopy (TEM) is used.[31] SDS-PAGE is used to determine the extent of covalent, disulfide linkages present in aggregates.[32] Extrinsic fluorescence spectroscopy with 8-anilino-1-naphthalene sulfonate (ANS) probe provides information concerning the surface hydrophobicity of aggregates.[33;34,35] FTIR provides insights into the secondary structure of native protein and aggregates in solution,[6,36-38] with the use of a FTIR microscope allowing for selection of individual protein particles for secondary structure analysis.[29]

This paper is a “protein particle formation” case study by utilizing a variety of analytical techniques to examine the effect of four different environmental stresses (freeze-thaw, shaking, stirring, and heating) and formulation composition (salt concentration) on the number, size range morphology, and compositional nature of the IgG1 aggregates/particles formed from stressing the mAb solutions. Additionally, a new data visualization method consisting of radar plot analysis was used to better evaluate the effects of environmental stress and salt concentration on particle size distributions as well as changes in certain morphological parameters measured by MFI. The trends observed in terms of types and amounts of particles formed under the different stress conditions are discussed, along with some comparisons to previous studies with different monoclonal antibodies.

## EXPERIMENTAL METHODS

### Materials

Purified monoclonal human IgG1 (mAb) was obtained from Janssen Biotech (Radnor, PA) at 40 mg/mL. The reagents and stir bars required for sample preparation were purchased from Sigma Aldrich (St. Louis, MO), and Fisher Scientific (Pittsburgh, PA). The 3 mL vials and rubber stoppers used to generate protein aggregates were purchased from West Pharmaceuticals (Lionville, PA). For counting and sizing of aggregates (using SEC, NTA, MFI, turbidity, visual assessments), the mAb was diluted to 1 mg/mL using 10 mM sodium acetate buffer, pH 5 ± 150 mM NaCl.[23] This condition was also used for morphological analysis of particles by MFI. For structural and morphological analysis of the aggregates (using TEM, MFI, SDS-PAGE, FTIR-Microscopy, ANS-Fluorescence), the mAb was diluted to 1 mg/ml in 10 mM sodium acetate buffer, pH 5 containing 150 mM NaCl.

### Generation of Aggregates

The 40 mg/mL IgG1 mAb solution was diluted to 1 mg/mL in 10 mM sodium acetate buffer, pH 5 ± 150 mM NaCl and then subjected to a variety of accelerated stress conditions. These conditions were selected to match pH solution conditions used previously with a different set of IgG mAbs[23,39] In each case, the buffer controls were stressed similarly to the protein

samples and analyzed using various sizing, counting, and characterization techniques. Since the buffer controls showed very low particle counts, the data were not included in the figures. For freeze-thaw stress, the mAb was frozen and thawed one to three times (indicated as cycles) at -80°C and room temperature, respectively (labeled FT-C1 and FT-C3). For shaking stress, the mAb was agitated at 300 rpm (using an IKA AS260.1 shaking platform) for 1-3 days (labeled shake-D1 and shake-D3). For stirring stress, the mAb was stirred at an intermediate speed (setting 5) on a stirring plate (ThermoSci Pierce Reacti-Therm III #18823 Heating/Stirring Module) using Flea Micro Teflon coated magnets (Fisher Scientific) for 1-3 days (labeled stir-D1 and stir-D3). For thermal stress, the mAb was incubated at 60°C in an incubator (Revco Ultima II) for 1-3 days (labeled heat-D1 and heat-D3).

### Size-Exclusion Chromatography

A Shimadzu Prominence HPLC system equipped with a diode-array detector was employed with a Tosoh Bioscience TSK-Gel Bioassist G3SW$_{XL}$ (7.8 mm × 30.0 cm) PEEK column and a corresponding PEEK Guard column (TSK Guard Column SW$_{XL,}$ 6.0 mm × 4.0 cm) that were preconditioned with BSA as described previously.[26] Molecular weight standards (Biorad Laboratories; Hercules, CA) were run to test for efficiency of separation and resolution. Both the column and guard column were equilibrated at 30°C for 1 hour using the mobile phase comprised of 0.2 M sodium phosphate, pH 6.8 at a flow rate of 0.7 ml/min. Aggregated samples were centrifuged at 16,000g (851 rotor on an IEC Micromax 3593) for 5 min and 10 μL of supernatant was injected for analysis and monitored simultaneously at 214 and 280 nm for each 30 min sample run.[26] Multimers, dimers, monomer, and fragment peaks were quantified using the LC Solutions data analysis software provided with the instrument as described elsewhere.[26]

### Nanoparticle Tracking Analysis (NTA)

Submicron (nanometer) sized particles were measured using a Nanosight LM-14 (Nanosight, Amesbury, UK) with a high resolution EMCCD camera. Stressed mAb solutions were centrifuged at 16,000g for 5 min and 300 uL of the supernatants were injected into the sample holder. The stirred (with and without NaCl) and heat stressed (with NaCl only) samples were diluted by a factor of 100 prior to analysis. Three 30 s movies were taken at ambient temperature for each sample at a viscosity of 0.95 cP. Data analysis was completed using NTA 2.3 software (Nanosight) with the required camera level and gain adjustments. Dilution factors were accounted for in the data analysis.

### Micro-Flow Digital Imaging

Subvisible (micron sized) protein particles were analyzed and imaged using a MFI DPA 4200 (Protein Simple, Santa Clara, CA). Prior to each analysis, the instrument was primed with purified water to obtain a particle-free baseline. Samples were gently swirled and 1 mL of each sample was removed using a low protein-binding pipette tip and loaded into a sample holder. Some of the samples (stir-D1 and D3 with and without NaCl; shake-D3 with NaCl; and heat-D3 with NaCl) were diluted by a factor of 100 prior to being passed through the instrument at a flow rate of 0.1m/min. The data were obtained as described previously by Kumru et al.[40]

### Data Visualization with Radar Plots

To generate MFI particle size distribution radar plots, subvisible particle concentrations and sizes for both unstressed and stressed samples were obtained from MFI's MVAS 1.3 software. Similarly, MFI particle morphology radar charts were created using the average mean intensity and aspect ratio values for each sample. All samples were run independently three times (n=3). The data were pre-processed in Excel and two radar plots (one showing average values and one showing variability in the runs) were generated using the MiddaughSuite software created in our lab.[41] The two radar charts were superimposed using Adobe Photoshop CS6. See Kalonia et al. 2013 and Kim et al. 2012 for a more detailed description of this data visualization methodology as applied to protein aggregation and conformational stability data, respectively.[41,42]

### SDS-PAGE

Samples were centrifuged at 16,000g for 5 min to separate the soluble fraction (supernatant) from the insoluble fraction (pellet). Both fractions were dissolved in NuPAGE LDS sample buffer (Life Technologies, Carlsbad, CA) with and without 50 mM DTT (BioRad) and incubated at 80°C for 90 s. Approximately 10 μg of each sample was separated on a 3-8% Tris-Acetate gel using Tris-Acetate running buffer (Life Technologies) for 65 min at 150V. A Hi-Mark unstained molecular weight ladder was used as a reference (Life Technologies). The starting protein concentration for the supernatant of one sample (stir-D3) was low so a maximum of 20 μL was loaded. Protein bands were visualized by staining with Bio-Safe Coomassie blue (BioRad).

### Turbidity

A HACH 2100 AN turbidimeter was used to monitor the turbidity of each of the samples. Prior to running the aggregated samples, NTU calibration standards were used to generate a standard curve.

### Transmission Electron Microscopy (TEM)

Carbon-coated grids were dipped into methylene chloride for 10 s to remove the top carbon layer and were dried for a few minutes. The images were obtained by uranyl acetate staining and by following the procedure by Kumru et al.[40]

### Free Thiol Quantitation

Samples were centrifuged at 16,000g for 5 min to separate the soluble (supernatant) and the insoluble (pellet) fractions. The pellet was dissolved in 6M guanidine hydrochloride (Fisher Scientific). The amount of free thiol in the samples as well as in the appropriate controls was measured using the protocol described in the Measure-iT Thiol Assay Kit (Molecular Probes) with a SpectraMax MS plate reader (Molecular Devices; Sunnyvale, CA).

### Extrinsic Fluorescence Spectroscopy

Samples were centrifuged at 16,000g for 5 min to separate the soluble and insoluble fractions. The pellet was resuspended in 10 mM sodium acetate, 150mM NaCl, pH 5. The protein concentration of each of these supernatant and pellet components was measured

using a Nanodrop spectrometer (Thermo Scientific) with light scattering correction. The samples were diluted to 0.1 mg/mL in 10 mM sodium acetate, 150 mM NaCl, pH 5. 8-Anilinonaphthalene-1-sulfonate (ANS; Sigma-Aldrich, St. Louis, MO) was added and the ANS fluorescence of the samples were recorded according to Kumru et al.[40] The signal from the buffer with equivalent amount of ANS was subtracted from all measurements.

### Fourier Transform Infrared Microscopy

Five μm gold filters (Pall Corporation) were used for analyzing the aggregated samples. Filters were equilibrated by washing with 0.1 M NaOH. The samples were then filtered, washed with ultrapure water, and dried overnight. A Bruker Hyperion FTIR Microscope with a 15X objective was used to image individual particles. Two-hundred-fifty-six scans were recorded from 600-4000 $cm^{-1}$ with a viewing area of about 100 μm × 100 μm. To observe the maximum change in secondary structure due to heating, a 1 mg/mL sample in acetate buffer (10 mM sodium acetate, 150 mM NaCl, pH 5) was heated for 20 min at 80°C. This heated sample (labeled heated control) was also filtered onto the 5 μm gold filter and dried overnight. OPUS (V6.5) software was used for baseline and atmospheric correction. The second derivative spectra were obtained using a nine-point Savitzky-Golay smoothing function.

### Fourier Transform Infrared Spectroscopy

The unstressed mAb at 1 and 10 mg/mL in 10 mM sodium acetate, 150 mM NaCl, pH 5 were analyzed with a Bruker Tensor 27 FTIR Spectrometer and a Bio-ATR cell. Two-hundred-fifty-six scans were recorded from 600-4000 $cm^{-1}$ at a resolution of 4 $cm^{-1}$. To observe changes in secondary structure as a function of temperature, 256 scans of 10 mg/mL of unstressed sample were heated from 10-87.5°C at 4 $cm^{-1}$ resolution and 120 s equilibration time with 2.5°C increments.

## RESULTS

### Counting and Sizing of Aggregates and Particles Formed under Accelerated Stress Conditions

**SEC (soluble aggregates, <100 nm)—**To determine the amount of smaller (soluble) nanometer aggregates, the stressed IgG1 mAb samples were centrifuged and the resulting supernatants were analyzed by SEC. The amount of protein material that did not elute from the SEC (referred to as insoluble aggregates) was indirectly determined by monitoring the decrease in the total area of the chromatogram peaks between unstressed (D0) and the stressed samples. The earliest eluted peak was labeled as multimer, the second peak as dimer, the third and largest peak as monomer, and the final peak as fragment based on the estimated molecular weights. In the absence of salt, heat stressed samples produced more fragments, dimers, and insoluble aggregates compared to the unstressed sample (Fig. 1A, I). Stirring formed more multimers and insoluble aggregates (Fig. 1G), while freeze-thaw formed a very small amount of multimers and dimers (Fig. 1A), compared to the unstressed sample. Shaking (Fig. 1E) did not show an increase in any species relative to the unstressed sample. In the presence of 0.15M NaCl, protein was further destabilized and generally resulted in the formation of more aggregates. Heat-stressed mAb in the presence of NaCl

(Fig. 1J) showed more insoluble aggregates, a larger decrease in monomer, and an increase in multimer compared to its NaCl-free counterpart, which showed some fragment formation and lower levels of impurity (Fig. 1I). Stirring the mAb solution in the presence of salt resulted in a large increase in insoluble aggregate and a concurrent decrease in monomer content (Fig. 1G vs. H). Freeze-thaw and shaking did not show changes in any species, but in the presence of NaCl, a slight increase in insoluble aggregate was observed (Fig 1D, 1F).

**Nanoparticle Tracking Analysis (NTA) (50-1000 nm particles)—**NTA was used to assess the concentration and size distribution of nanometer sized particles (also referred to as submicron particles) formed in stressed and unstressed samples. Stirring of the mAb solution in the absence of NaCl (Fig. 2A and 2C) generated the largest number of nanometer sized particles (between ~150-250 nm). In contrast, in the presence of salt, heating generated the most nanometer sized particles (Fig. 2B and 2D). The concentration of nanometer particles present in the unstressed controls was below the instrument's quantitation limit (data not shown).

**MFI (2-100 μm particles)—**Subvisible particle data (concentration and size range of micron size particles) obtained from MFI measurements of stressed and unstressed samples were visualized using radar plots (Fig. 3 and Supplemental Fig. S1). This novel data visualization method for MFI data is described in detail elsewhere.[42] As shown in the key to Figure 3, the concentric circles represent concentration of particles, with the lowest concentration ($10^2$) being the innermost circle, and highest concentration ($>10^7$) being the outermost. The 5 corners of the polygon within the circles represent the particle size bins. An increase in size of the polygon towards one corner represents an increase in concentration of particles in that size bin (e.g., stretching of a corner from the innermost concentric circle to the outermost circle in size bin number 3 indicates that there is an increase in the ≥10<25 μm particles from $10^2$ to $>10^7$ particles/mL).

As shown in Figure 3, the size and concentration of subvisible particles formed is highly dependent on the type of stress. In the absence of NaCl, freeze-thaw and heat stressed mAb samples showed the lowest concentration of particles even after 3 cycles/days of stress, while shaking and stirring showed a higher concentration of particles. Stirring produced the most subvisible particles, especially in the 2-25 μm size range. In the presence of NaCl, a higher concentration of particles, especially in the 2-25 μm size range, was observed in all of the stressed mAb samples. The heated mAb showed a large difference in both particle number and size in the presence and absence of salt that increased from day 1 to day 3. A large variability in the larger particles was observed (the lighter shading on the radar plots reflects the standard deviation of the measurements). In general, shaking the mAb solution containing NaCl generated the largest subvisible particles (2-50 μm) (Fig. 3). Particle counts of controls were negligible.

**Turbidity and Visual Assessment—**Results of turbidity measurements and visual observations of the stressed mAb solutions are shown in Table 1. In samples lacking NaCl, agitation and stirring resulted in the highest number of >100 μm (referred to as visible particles, VP), with stirring producing the greatest turbidity. No major NaCl effect was seen for the freeze-thaw stress. Agitation, stirring, and heating stresses on the mAb formed more

VP and higher turbidity in the presence of NaCl than in the absence of it. The highest turbidity levels were measured for stir-D3 samples, followed by stir-D1, and heat-D3. In addition, the presence of NaCl increased the turbidity for the heated (heat-D1 and heat-D3) protein compared to the corresponding heat stressed mAb samples without NaCl. Shaken or stirred mAb samples formed a large number of visible particles regardless of the presence or absence of NaCl.

## Structural Characterization of Aggregates and Particles

**Particle Morphology—**As an initial step in characterizing the nature and composition of the particles formed under different stresses, MFI was used to elucidate morphological information (intensity and aspect ratio parameters) of the subvisible particles generated after three days of stress (Fig. 3 and Supplemental Fig. S1). Aspect ratio is a ratio of width of the particle relative to the height and intensity is related to the particle absorption characteristics. Data were visualized in the form of a radar plot (Fig. 4). Figure 4 shows the different stresses applied to mAb solutions with and without NaCl on the x-axis and the MFI morphology parameters, intensity and aspect ratio, on the y-axis. The top and bottom radar charts describe the intensity and aspect ratio, respectively, of the particles as a function of stress and solution condition. As shown in the key to Figure 4, the aspect ratio of the micron particles varies from ~0.35 (elongated) to 0.85 (more circular) and the intensity from about 350 (opaque) to 850 (highly transparent) intensity level units (ILU). It should be emphasized that the concentric circles here do not represent concentration, but rather a change in particle morphology with the outermost circle representing elongated, opaque particles, and the innermost circle representing transparent, circular particles. The corners of the 5-sided polygon represent distinct particle size bins (labeled 1-5 in the figure). The pink-shaded region indicates that an insufficient number of particles were collected in that size range for accurate morphological analysis.

In the absence of NaCl, the shaking of the mAb solution over 3 days resulted in particles that appeared transparent (Fig. 4A) and elongated (Fig. 4B) over all particle size ranges. In the presence of NaCl under the same stress condition, the particles formed are less transparent (i.e., more opaque) and less elongated (i.e., more circular in shape) over a narrower size range. Stirring-induced mAb particles formed in the presence or absence of NaCl do not show notable differences in intensity or aspect ratio. The concentration of particles in the freeze-thaw and heated samples without NaCl was lower (Fig. 3) and an accurate comparison of the morphology change across the size ranges was limited (as shown by the shaded areas in Figure 4).

To characterize the morphology of smaller particles, TEM was used to examine the shape of nanometer sized aggregates generated from 3 days of different stresses in the presence of 0.15 M NaCl. Some representative TEM images are shown in Figure 5. It can be seen that the type of stress to which the mAb solution was subjected influences the morphology of the aggregates generated. Freeze-thaw and heated aggregates appear very fibrillar, while agitated-induced aggregates appear fibrillar with some spherical aggregates. The stirring-induced aggregates were predominantly spherical in nature in this size range.

**Non-native disulphide cross-linking—**SDS-PAGE was used to study the formation of non-native covalent crosslinking in the stressed mAb. Results for the stirring and heating stressed mAb containing NaCl are shown in Figure 6A and B (non-reduced and reduced, respectively). These samples were first centrifuged to separate the supernatant (S) and pellet components (P) prior to electrophoresis. The non-reduced supernatants contained predominantly monomers while the pellets contained high molecular weight species above 500 kDa (i.e., larger than tetramer). Upon reduction of the supernatant and pellet, a complete loss in the high molecular weight material was observed with the light and heavy chains bands of the mAb visible as the primary species. The pellet for stir-D1 and D3, heat-D1 and D3 contained significant amounts of non-native disulfide linked aggregates. The supernatant of heat-D1 protein contained some of these non-native disulfide linked aggregates as well. No disulfide-linked aggregates were detected in freeze-thaw and agitation stressed mAb samples (data not shown). The number of free sulfhydryl groups in the mAb samples was also measured, and virtually no free thiols were present in control or stressed samples (data not shown).

**Overall secondary structure content—**The secondary structure of the aggregated samples was studied using FTIR spectroscopy of control mAb samples and FTIR microscopy of individual particles formed by stress in 10 mM acetate, 150 mM NaCl, pH 5. Representative spectra are shown in Figure 7 along with wavelength values from multiple measurements including standard deviations. Two mAb controls were prepared for comparison to the particles formed from stressed samples: an unstressed mAb with native conformation (Figure 7A in the form of second derivative FTIR spectra) and particles isolated from an extensively heated mAb sample with some degree of structural perturbations (Figure 7B). Figures C-F show microscopic images and the corresponding FTIR spectra of isolated amorphous mAb particles generated under different stresses.

In the Amide I region of the second derivative FTIR spectra of the native mAb, two minima at 1637 $cm^{-1}$ and 1690 $cm^{-1}$ were observed (Figure 7A). This result is consistent with the predominantly intramolecular beta sheets present in native IgGs. [9,43,44] For the isolated mAb particles from the extensively heat stressed control, severely altered secondary structure displaying extensive loss of intramolecular beta sheet structure (as shown by loss of the two minima seen in the native mAb control, and the appearance of intermolecular beta sheets with minima at 1617 $cm^{-1}$, and 1693 $cm^{-1}$ (Figure 7B) is seen. For the isolated mAb particles produced by three days of heating at 60°C, the spectra show the sample is more similar to the extensively heated control as evidenced by the presence of the two minima at 1624 $cm^{-1}$ and 1694 $cm^{-1}$.[45,46] The mAb particles isolated after three freeze-thaw cycles and three days of agitation have FTIR spectra with primarily native-like structure as seen by the second derivative minima at 1634 $cm^{-1}$ and 1691 $cm^{-1}$ and 1635 $cm^{-1}$ and 1692 $cm^{-1}$, respectively. The stirred aggregates show reproducibly shifted minima in the main second derivative peak to 1631 $cm^{-1}$ indicating some alteration in secondary structure.

**Surface hydrophobicity—**To examine any changes in the exposure of apolar regions in the stressed samples containing NaCl due to structural perturbations or aggregation/self-association, ANS extrinsic fluorescence spectroscopy was used. Stress induced aggregated

mAb samples were centrifuged and separated into supernatant and pellet components. They were analyzed along with two controls: the unstressed mAb (D0) and a positive control (Heat-melt). As a positive control to determine the greatest extent of apolar binding of ANS, the mAb solution was heated from 10 to 87.5°C in the presence of ANS. From the emission spectrum, it was determined that the maximum binding of ANS to the mAb occurred at 72°C suggesting maximal ANS access to apolar sites at high temperature. Representative spectra are shown in Figure 8. The control mAb solution (D0) along with supernatants from the FT, shake, and stir-D1 samples (Fig. 8A,B) show very little fluorescence intensity indicating that in these samples, ANS has very little access to the apolar regions of the mAb. In the stir-D1 pellet, slightly higher fluorescence intensity was observed, which suggests some exposure of apolar sites in these aggregates (Fig. 8A, B). The heat-D1 supernatant and pellet show the largest ANS fluorescence intensity increase suggesting the greatest exposure of apolar regions. The heat stressed mAb samples containing NaCl displayed a similar magnitude of fluorescence intensity as the positive control (heat-melt) indicating that this stress condition may also generate samples with extensively apolar exposed regions.

## DISCUSSION

As an initial set of experiments, we first counted and sized protein particles generated under accelerated stress conditions employing an IgG1 mAb solution with and without 0.15 M NaCl. A summary of the counting and sizing results from SEC, NTA, MFI, Turbidity, and Visual Assessments are presented in Table 2. Different stresses (in the presence and absence of NaCl) result in the formation of mAb aggregates and particles of varying sizes which cannot be measured by a single analytical method. As shown in Table 2, using multiple techniques is therefore very important for analyzing the formation of a broad size range of aggregates. For example, SEC showed that the formation of soluble aggregates was influenced by the presence of NaCl across the four stresses. NTA results demonstrated that the presence of NaCl affected the extent of nanometer particle formation in the freeze-thaw and heat stressed samples, but not for the agitated and stirred stressed samples. Similarly, MFI detected that NaCl enhanced the formation of micron particles only for the freeze-thaw stressed mAb sample. Finally, turbidity and visual assessments showed changes in particle formation (due to the presence or absence of NaCl) with heat stressed mAb solutions.

Freeze-thaw stress was observed to be the mildest condition in solutions without NaCl since essentially no detectable aggregates or particles were seen (Table 2, first row). Upon addition of NaCl (Table 2, second row), some insoluble aggregates (detected as a loss of total mass by SEC) and some nanometer and micron particles were detected by NTA and MFI. Shaking the mAb solution with and without NaCl (third and fourth row in Table 2) generated a turbid solution with primarily micron (2 to >100 μm) size particles observed by MFI and visual inspection. The shaken solution in presence of NaCl was more turbid with some insoluble aggregates, and a larger number of micron-sized particles 2 to >100 μm. Stirring without NaCl produced a moderately turbid solution consisting of some insoluble aggregates, submicron, micron, as well as a large number of visible entities. Stirring the mAb solutions, in the presence of NaCl, generated the most turbid solutions consisting of a very large amount of insoluble aggregates (20% after day 1 and around 60% after 3 days of stress, as quantified by SE-HPLC). The largest differences in aggregate and particle

formation were observed due to heating the mAb solution (Table 2; rows seven and eight). Heating in the absence of NaCl generated a fairly clear solution consisting of primarily monomers with a very small amount of insoluble aggregates and fragments (SEC), little to no nanometer-sized (NTA), micron (MFI), and visible particles even after three days of stress. In the presence of NaCl, however, a highly turbid solution formed containing much more insoluble and multimer aggregates as well as a large increase in the number of nanometer, micron, and visible sized particles.

Comparison of these results to other studies shows similar trends in which mAb aggregate and particle formation depends on the type of stress and solution conditions. For an IgG1 mAb with a basic pI range formulated at lower solution pH such as pH 5.0, the addition of NaCl (<0.15 M) may promote protein aggregation and particle formation during environmental stress by a combination of effects resulting from neutralizing protein surface charge and decreasing electrostatic interactions. These effects may promote protein-protein interactions (colloidal stability) or decrease the structural integrity and stability of the protein (conformational stability).[9,47] The last column of Table 2 describes the impact of NaCl on various stresses using eight analytical readouts obtained from four instruments. For a given stress, column values can potentially range from 0/8, indicating NaCl had no impact on the aggregation behavior, to 8/8 where NaCl impacted the aggregation behavior of the mAb as measured by all of these analytical methods. Agitation and stirring stresses of the mAb solution were least influenced by the presence of NaCl (1 out of 8). Although the two stresses themselves were damaging to the protein, the addition of NaCl minimally increased mAb instability (as manifested in detectable changes in SEC for percent insoluble aggregate and monomer content for agitation and stirring stresses, respectively). Aggregation of the mAb under freeze-thaw stress was more influenced by the presence of NaCl (3 out of 8). Although freeze-thaw stress does not seem to cause alterations in the conformation of the mAb (see below), increases in percent insoluble and soluble aggregate, as well as nanometer and micron sized particles (by SEC, NTA, and MFI, respectively) were noted due to the presence of NaCl, indicating decreased colloidal stability. Finally, heat stress showed the largest effect of NaCl on mAb instability (6 out of 8). While heating of the mAb solution in the absence of salt alters the conformational stability of the protein, it does not result in extensive aggregate or particle formation. With the addition of NaCl, however, there is now a large colloidal component to the mAb instability.

Despite the availability of new analytical methods to accurately and precisely count and size protein particles in the submicron and subvisible size range,[27,28,48-51] biophysical characterization of the nature, composition and structural integrity of the protein within these particles remains a major analytical challenge. The focus of this work was to characterize aggregates and particles formed in an IgG1 mAb in the presence of 0.15M NaCl as a function of various stresses (freeze-thaw, shaking, stirring and heating). The primary goal was to characterize the morphology, structural integrity and composition of the IgG1 particles formed in 0.15M NaCl containing solutions by probing the extent of non-native covalent cross-linking, changes in overall protein secondary structure, and alterations in surface hydrophobicity within the particles as formed by each type of stress applied to the mAb solutions. Additionally, we also evaluated the morphology of these particles by TEM and by a newly developed approach from our laboratory to analyze MFI size distribution

and morphological data using radar plots.[42] These plots are commonly used to summarize large sets of protein data from multiple biophysical techniques. Radar plots are used to better visualize particle size distribution and morphological parameters of the particles.[42]

The freeze-thaw stress appeared to be mild and essentially did not change the overall higher order structure or covalent crosslinking of the protein within the aggregates. Particles, isolated onto a gold filter, showed no detectable alterations in overall secondary structure relative to the native IgG sample, even after three freeze thaw cycles. The nanometer sized aggregates appeared to have a fibrillar morphology by TEM. The micron sized particles (10-50μm) were opaque (less transparent) and more elongated. Similarly, freeze-thaw samples showed very low surface hydrophobicity almost equal to that of the native protein. There appeared to be no covalent cross-linking present in the sample and no corresponding higher molecular weight aggregates seen on SDS-PAGE gels (data not shown). Results obtained from similar experiments by Joubert et al. as well as Barnard et al and Zhang et al.[52,53] with different mAbs were consistent with our observations.[23]

For mAb solutions stressed by shaking, a common stress encountered by many protein drugs during transportation, generated predominantly fibrillar and slightly spherical nanometer particles, while the micron sized particles were more opaque and circular than the samples shaken without NaCl, as shown in Figures 4 and 5. These stressed samples contained little to no covalently linked aggregates with largely native-like secondary structure and low surface hydrophobicity (Figs 6-8) even after three days of shaking stress. While shaking generated higher number of aggregates and particles than freeze-thaw, there were not many differences in the biophysical characteristics of the aggregates generated by these two stresses compared to the unstressed, native protein. This result is similar to data published previously with other proteins.[17,23,54]

Stirring stress was a harsher condition on the IgG1 compared to freeze-thaw and shaking. In addition, the particles generated from this stress were predominantly spherical in morphology which was not observed with other stresses. From the MFI morphology data, NaCl did not notably affect particle morphology (in terms of aspect ratio and intensity) of the stirred samples in the micron size range as shown by the radar chart analysis in Figure 4. Biophysical differences were also observed in protein from the pellet fraction and supernatant fraction of the centrifuged stirred IgG mAb samples. The protein in the pellet fraction displayed greater surface hydrophobicity (Figure 8) and contained an increased amount of reducible high molecular weight covalently linked aggregates (Figure 6) than the supernatant fraction. The ANS fluorescence data suggest that the population of aggregates present in the pellet may be more structurally altered compared to the aggregates present in the supernatant. The isolated stir-stressed particles showed some loss in overall intramolecular beta sheet structure content and some increase in the formation of intermolecular beta sheet structures (non-native, aggregated structures) as shown by FTIR analysis (Figure 7). One study reported that the overall secondary structure of the stirred sample was similar to that of the unstressed sample, contrary to our results with this IgG.[17] In addition to rapid transportation of aggregates into bulk solution from the interface, protein also encounters the harsh shear force of the stir-bar and the resulting thermal effects as well

as cavitation.[17,55] All of these factors could account for higher aggregation and particulation with stirring stress compared to shaking.

For the heated samples of the IgG mAb, the supernatant fraction contained less non-native covalently linked aggregates compared to the pellet fraction which possessed higher levels of this type of disulfide cross-linked aggregate as measured by SDS-PAGE (Figure 6). The variability in the micron particle concentration was very high due to heating, so it is difficult to make definitive conclusions about the aspect ratio or intensity of these particles, although more elongated and more opaque particles were seen in the presence of NaCl (Figure 4). In the presence of NaCl, nanometer sized particles seen by TEM appeared fibrillar in morphology (Figure 5). The heat stressed samples displayed a highly perturbed overall secondary structure content consisting of predominantly intermolecular beta sheets as measured by FTIR (Figure 7). The increased ANS binding in both the supernatant and pellet of the centrifuged heated samples suggests significant exposure of apolar moieties in both fractions. Hawe et al. noted that the heat generated aggregates contained non-native covalent cross-linking with significantly increased ANS binding (increase in surface hydrophobicity), as well as a large perturbation in the secondary structure [18,23] Zhang et al. conducted a similar experiment with Bevacizumab and determined that heat generated aggregates had significantly altered structure from their ANS and intrinsic Trp fluorescence data.[53] These results are consistent with our observations

In summary, while there has been a vast growth in our ability to count and size protein aggregates and particles over a wide size range during the past ~5 years, our analytical capabilities to describe the morphology, structural integrity and composition of the protein within these particles is still limited. The goal of this study was to provide a case study to examine the effect of different environmental stresses on an IgG1 mAb solution in terms of the morphology of particles formed as well the extent of structural alterations of the protein within the particles. We confirmed results of previous studies [17,18,23,52,55] that the type of stress a mAb solution experiences greatly influences many of its physical properties in distinct ways. There are still many gaps in our understanding that need to be addressed, [56] especially if there is a relationship between a particular particle count, particle size range, particle weight or perhaps the physicochemical or morphological trait(s) of protein particles/ aggregates and their potential to generate an immune response *in vivo*. [56-62]

## Supplementary Material

Refer to Web version on PubMed Central for supplementary material.

## Acknowledgments

The authors wish to thank and acknowledge Janssen R&D for providing the IgG1 mAb for this study and the Kansas Bioscience Authority for financial support. ST financial support was provided by NIH biotechnology training grant 5-T32-GM008359. We would also like to thank Dr. Prem Thapa, Dr. David Moore, and Heather Shinogle of the KU Microscopy and Analytical Imaging Laboratory for helping us obtain TEM images.

## References


1. Hermeling S, Crommelin DJ, Schellekens H, Jiskoot W. Structure-immunogenicity relationships of therapeutic proteins. Pharm Res. 2004; 21(6):897–903. [PubMed: 15212151]
2. Rosenberg AS. Effects of protein aggregates: an immunologic perspective. Aaps J. 2006; 8(3):E501–507. [PubMed: 17025268]
3. Schellekens H. Bioequivalence and the immunogenicity of biopharmaceuticals. Nat Rev Drug Discov. 2002; 1(6):457–462. [PubMed: 12119747]
4. Schellekens H. Immunogenicity of therapeutic proteins. Nephrol Dial Transplant. 2003; 18(7): 1257–1259. [PubMed: 12808158]
5. Cromwell ME, Hilario E, Jacobson F. Protein aggregation and bioprocessing. Aaps J. 2006; 8(3):E572–579. [PubMed: 17025275]
6. Mahler HC, Friess W, Grauschopf U, Kiese S. Protein aggregation: pathways, induction factors and analysis. J Pharm Sci. 2009; 98(9):2909–2934. [PubMed: 18823031]
7. Wang W. Protein aggregation and its inhibition in biopharmaceutics. Int J Pharm. 2005; 289(1-2):1–30. [PubMed: 15652195]
8. Shire SJ, Shahrokh Z, Liu J. Challenges in the development of high protein concentration formulations. J Pharm Sci. 2004; 93(6):1390–1402. [PubMed: 15124199]
9. Chi EY, Krishnan S, Randolph TW, Carpenter JF. Physical stability of proteins in aqueous solution: mechanism and driving forces in nonnative protein aggregation. Pharm Res. 2003; 20(9):1325–1336. [PubMed: 14567625]
10. Arosio P, Rima S, Morbidelli M. Aggregation mechanism of an IgG2 and two IgG1 monoclonal antibodies at low pH: from oligomers to larger aggregates. Pharm Res. 2013; 30(3):641–654. [PubMed: 23054090]
11. Strambini GB, Gonnelli M. Protein stability in ice. Biophys J. 2007; 92(6):2131–2138. [PubMed: 17189314]
12. Pikal-Cleland KA, Cleland JL, Anchordoquy TJ, Carpenter JF. Effect of glycine on pH changes and protein stability during freeze-thawing in phosphate buffer systems. J Pharm Sci. 2002; 91(9): 1969–1979. [PubMed: 12210044]
13. Kreilgaard L, Frokjaer S, Flink JM, Randolph TW, Carpenter JF. Effects of additives on the stability of recombinant human factor XIII during freeze-drying and storage in the dried solid. Arch Biochem Biophys. 1998; 360(1):121–134. [PubMed: 9826437]
14. Hillgren A, Lindgren J, Alden M. Protection mechanism of Tween 80 during freeze-thawing of a model protein, LDH. Int J Pharm. 2002; 237(1-2):57–69. [PubMed: 11955804]
15. Kueltzo LA, Wang W, Randolph TW, Carpenter JF. Effects of solution conditions, processing parameters, and container materials on aggregation of a monoclonal antibody during freeze-thawing. J Pharm Sci. 2008; 97(5):1801–1812. [PubMed: 17823949]
16. Wang, W.; Roberts, CJ., editors. Aggregation of Therapeutic Proteins. Hoboken, NJ: Wiley; 2010.
17. Kiese S, Papppenberger A, Friess W, Mahler HC. Shaken, not stirred: mechanical stress testing of an IgG1 antibody. J Pharm Sci. 2008; 97(10):4347–4366. [PubMed: 18240293]
18. Hawe A, Kasper JC, Friess W, Jiskoot W. Structural properties of monoclonal antibody aggregates induced by freeze-thawing and thermal stress. Eur J Pharm Sci. 2009; 38(2):79–87. [PubMed: 19540340]
19. Eppler A, Weigandt M, Hanefeld A, Bunjes H. Relevant shaking stress conditions for antibody preformulation development. Eur J Pharm Biopharm. 2010; 74(2):139–147. [PubMed: 19922795]
20. Brych SR, Gokarn YR, Hultgen H, Stevenson RJ, Rajan R, Matsumura M. Characterization of antibody aggregation: role of buried, unpaired cysteines in particle formation. J Pharm Sci. 2010; 99(2):764–781. [PubMed: 19691118]
21. Wang W, Nema S, Teagarden D. Protein aggregation--pathways and influencing factors. Int J Pharm. 2010; 390(2):89–99. [PubMed: 20188160]
22. Hawe A, Wiggenhorn M, van de Weert M, Garbe JH, Mahler HC, Jiskoot W. Forced degradation of therapeutic proteins. J Pharm Sci. 2012; 101(3):895–913. [PubMed: 22083792]

23. Joubert MK, Luo Q, Nashed-Samuel Y, Wypych J, Narhi LO. Classification and characterization of therapeutic antibody aggregates. J Biol Chem. 2011; 286(28):25118–25133. [PubMed: 21454532]
24. Demeule B, Messick S, Shire SJ, Liu J. Characterization of particles in protein solutions: reaching the limits of current technologies. Aaps J. 2010; 12(4):708–715. [PubMed: 20953747]
25. Narhi LO, Schmit J, Bechtold-Peters K, Sharma D. Classification of protein aggregates. J Pharm Sci. 2012; 101(2):493–498. [PubMed: 21989781]
26. Bond MD, Panek ME, Zhang Z, Wang D, Mehndiratta P, Zhao H, Gunton K, Ni A, Nedved ML, Burman S, Volkin DB. Evaluation of a dual-wavelength size exclusion HPLC method with improved sensitivity to detect protein aggregates and its use to better characterize degradation pathways of an IgG1 monoclonal antibody. J Pharm Sci. 2010; 99(6):2582–2597. [PubMed: 20039394]
27. Wang, T.; Joshi, SB.; Kumru, OS.; Telikepalli, S.; Middaugh, CR.; Volkin, DB. Case Studies Applying Biophysical Techniques to Better Characterize Protein Aggregates and Particulates of Varying Size. In: Narhi, LO., editor. Biophysics for Therapeutic Protein Development. Springer; 2013. p. 205-243.
28. Zolls S, Tantipolphan R, Wiggenhorn M, Winter G, Jiskoot W, Friess W, Hawe A. Particles in therapeutic protein formulations, Part 1: overview of analytical methods. J Pharm Sci. 2012; 101(3):914–935. [PubMed: 22161573]
29. Wuchner K, Buchler J, Spycher R, Dalmonte P, Volkin DB. Development of a microflow digital imaging assay to characterize protein particulates during storage of a high concentration IgG1 monoclonal antibody formulation. J Pharm Sci. 2010; 99(8):3343–3361. [PubMed: 20229596]
30. Sharma DK, Oma P, Pollo MJ, Sukumar M. Quantification and characterization of subvisible proteinaceous particles in opalescent mAb formulations using micro-flow imaging. J Pharm Sci. 2010; 99(6):2628–2642. [PubMed: 20049937]
31. Ohno O, Cooke TD. Electron microscopic morphology of immunoglobulin aggregates and their interactions in rheumatoid articular collagenous tissues. Arthritis Rheum. 1978; 21(5):516–527. [PubMed: 666872]
32. Flatman S, Alam I, Gerard J, Mussa N. Process analytics for purification of monoclonal antibodies. J Chromatogr B Analyt Technol Biomed Life Sci. 2007; 848(1):79–87.
33. Piekarska B, Skowronek M, Rybarska J, Stopa B, Roterman I, Konieczny L. Congo red-stabilized intermediates in the lambda light chain transition from native to molten state. Biochimie. 1996; 78(3):183–189. [PubMed: 8831949]
34. Hawe A, Sutter M, Jiskoot W. Extrinsic fluorescent dyes as tools for protein characterization. Pharm Res. 2008; 25(7):1487–1499. [PubMed: 18172579]
35. He F, Phan DH, Hogan S, Bailey R, Becker GW, Narhi LO, Razinkov VI. Detection of IgG aggregation by a high throughput method based on extrinsic fluorescence. J Pharm Sci. 2010; 99(6):2598–2608. [PubMed: 20039384]
36. Schule S, Friess W, Bechtold-Peters K, Garidel P. Conformational analysis of protein secondary structure during spray-drying of antibody/mannitol formulations. Eur J Pharm Biopharm. 2007; 65(1):1–9. [PubMed: 17034996]
37. Matheus S, Mahler HC, Friess W. A critical evaluation of Tm(FTIR) measurements of high-concentration IgG1 antibody formulations as a formulation development tool. Pharm Res. 2006; 23(7):1617–1627. [PubMed: 16783474]
38. Vermeer AW, Bremer MG, Norde W. Structural changes of IgG induced by heat treatment and by adsorption onto a hydrophobic Teflon surface studied by circular dichroism spectroscopy. Biochim Biophys Acta. 1998; 1425(1):1–12. [PubMed: 9813217]
39. Luo Q, Joubert MK, Stevenson R, Ketchem RR, Narhi LO, Wypych J. Chemical modifications in therapeutic protein aggregates generated under different stress conditions. J Biol Chem. 2011; 286(28):25134–25144. [PubMed: 21518762]
40. Kumru OS, Liu J, Ji JA, Cheng W, Wang YJ, Wang T, Joshi SB, Middaugh CR, Volkin DB. Compatibility, physical stability, and characterization of an IgG4 monoclonal antibody after dilution into different intravenous administration bags. J Pharm Sci. 2012; 101(10):3636–3650. [PubMed: 22733600]

41. Kim JH, Iyer V, Joshi SB, Volkin DB, Middaugh CR. Improved data visualization techniques for analyzing macromolecule structural changes. Protein Sci. 2012; 21(10):1540–1553. [PubMed: 22898970]
42. Kalonia C, Kumru OS, Kim JH, Middaugh CR, Volkin DB. Radar Chart Array Analysis to Visualize Effects of Formulation Variables on IgG1 Particle Formation as Measured by Multiple Analytical Techniques. J Pharm Sci. 2013
43. Chi EY, Krishnan S, Kendrick BS, Chang BS, Carpenter JF, Randolph TW. Roles of conformational stability and colloidal stability in the aggregation of recombinant human granulocyte colony-stimulating factor. Protein Sci. 2003; 12(5):903–913. [PubMed: 12717013]
44. Vonhoff S, Condliffe J, Schiffter H. Implementation of an FTIR calibration curve for fast and objective determination of changes in protein secondary structure during formulation development. J Pharm Biomed Anal. 2010; 51(1):39–45. [PubMed: 19726151]
45. Murphy BM, Zhang N, Payne RW, Davis JM, Abdul-Fattah AM, Matsuura JE, Herman AC, Manning MC. Structure, stability, and mobility of a lyophilized IgG1 monoclonal antibody as determined using second-derivative infrared spectroscopy. J Pharm Sci. 2012; 101(1):81–91. [PubMed: 21918984]
46. van Stokkum IH, Linsdell H, Hadden JM, Haris PI, Chapman D, Bloemendal M. Temperature-induced changes in protein structures studied by Fourier transform infrared spectroscopy and global analysis. Biochemistry. 1995; 34(33):10508–10518. [PubMed: 7654705]
47. Hamada H, Arakawa T, Shiraki K. Effect of additives on protein aggregation. Curr Pharm Biotechnol. 2009; 10(4):400–407. [PubMed: 19519415]
48. Weinbuch D, Zolls S, Wiggenhorn M, Friess W, Winter G, Jiskoot W, Hawe A. Micro-flow imaging and resonant mass measurement (archimedes) - complementary methods to quantitatively differentiate protein particles and silicone oil droplets. J Pharm Sci. 2013; 102(7):2152–2165. [PubMed: 23625851]
49. Hawe A, Romeijn S, Filipe V, Jiskoot W. Asymmetrical flow field-flow fractionation method for the analysis of submicron protein aggregates. J Pharm Sci. 2012; 101(11):4129–4139. [PubMed: 22911663]
50. Wilson GA, Manning MC. Flow imaging: moving toward best practices for subvisible particle quantitation in protein products. J Pharm Sci. 2013; 102(3):1133–1134. [PubMed: 23303598]
51. Hamrang Z, Rattray NJ, Pluen A. Proteins behaving badly: emerging technologies in profiling biopharmaceutical aggregation. Trends Biotechnol. 2013
52. Barnard JG, Singh S, Randolph TW, Carpenter JF. Subvisible particle counting provides a sensitive method of detecting and quantifying aggregation of monoclonal antibody caused by freeze-thawing: insights into the roles of particles in the protein aggregation pathway. J Pharm Sci. 2011; 100(2):492–503. [PubMed: 20803602]
53. Zhang A, Singh SK, Shirts MR, Kumar S, Fernandez EJ. Distinct aggregation mechanisms of monoclonal antibody under thermal and freeze-thaw stresses revealed by hydrogen exchange. Pharm Res. 2012; 29(1):236–250. [PubMed: 21805212]
54. Serno T, Carpenter JF, Randolph TW, Winter G. Inhibition of agitation-induced aggregation of an IgG-antibody by hydroxypropyl-beta-cyclodextrin. J Pharm Sci. 2010; 99(3):1193–1206. [PubMed: 19774651]
55. Mahler HC, Muller R, Friess W, Delille A, Matheus S. Induction and analysis of aggregates in a liquid IgG1-antibody formulation. Eur J Pharm Biopharm. 2005; 59(3):407–417. [PubMed: 15760721]
56. Bee JS, Goletz TJ, Ragheb JA. The future of protein particle characterization and understanding its potential to diminish the immunogenicity of biopharmaceuticals: a shared perspective. J Pharm Sci. 2012; 101(10):3580–3585. [PubMed: 22736570]
57. Ripple DC, Dimitrova MN. Protein particles: what we know and what we do not know. J Pharm Sci. 2012; 101(10):3568–3579. [PubMed: 22736521]
58. Rosenberg AS, Verthelyi D, Cherney BW. Managing uncertainty: a perspective on risk pertaining to product quality attributes as they bear on immunogenicity of therapeutic proteins. J Pharm Sci. 2012; 101(10):3560–3567. [PubMed: 22736548]

59. Marszal E, Fowler E. Workshop on predictive science of the immunogenicity aspects of particles in biopharmaceutical products. J Pharm Sci. 2012; 101(10):3555–3559. [PubMed: 22736535]

60. Wang W, Singh SK, Li N, Toler MR, King KR, Nema S. Immunogenicity of protein aggregates--concerns and realities. Int J Pharm. 2012; 431(1-2):1–11. [PubMed: 22546296]

61. Joubert MK, Hokom M, Eakin C, Zhou L, Deshpande M, Baker MP, Goletz TJ, Kerwin BA, Chirmule N, Narhi LO, Jawa V. Highly aggregated antibody therapeutics can enhance the in vitro innate and late-stage T-cell immune responses. J Biol Chem. 2012; 287(30):25266–25279. [PubMed: 22584577]

62. Filipe V, Jiskoot W, Basmeleh AH, Halim A, Schellekens H. Immunogenicity of different stressed IgG monoclonal antibody formulations in immune tolerant transgenic mice. MAbs. 2012; 4(6)

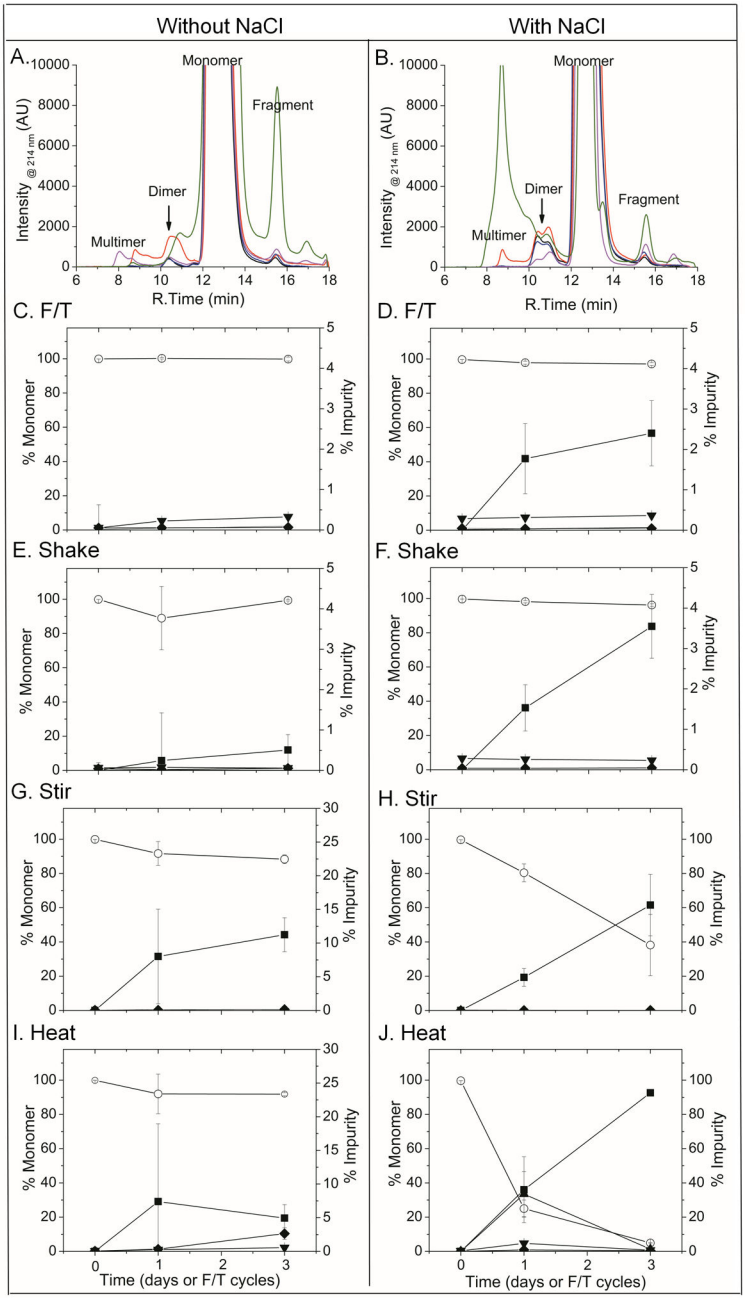


**Figure 1.**

Formation of soluble and insoluble aggregates in IgG1 mAb solutions exposed to different stresses as measured by SEC. (A, B) Representative SEC chromatograms monitored at 214 nm of 1 mg/mL antibody in 10 mM sodium acetate, pH 5 in absence (A) and presence (B) of 150 mM NaCl. Key: Day 0 Control (—), F/T Cycle 3 ( ), Agitation Day 3 ( ), Stirring Day 3 ( ), Heating Day 3 ( ). Plots of monomer loss and changes in amounts of impurities as a function of different stresses are shown: freeze-thaw cycles (C) without NaCl and (D) with NaCl; days of agitation (E) without NaCl and (F) with NaCl; days of stirring (G) without NaCl and (H) with NaCl; days of heating (I) without NaCl and (J) with

NaCl. Key for C-J: ⬭ -% Monomer; Impurity:▬- % Insoluble; ▲- % Multimer; ▼ - % Dimer; ◆- % Fragment. Each graph represents the average of three separate experiments (n=3). Error bars represent the 95% confidence interval.

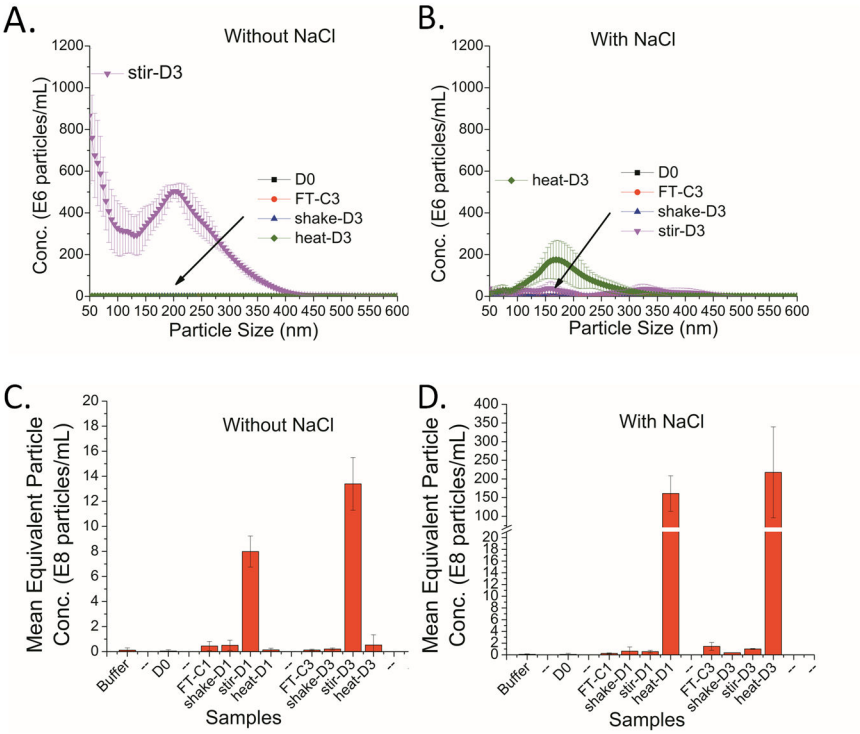


**Figure 2.**

Formation of submicron sized particles in IgG1 mAb solutions exposed to different stresses as measured by NTA. Representative NTA data showing the formation of nanometer sized particles due to four indicated stresses applied to 1 mg/mL antibody solution containing 10 mM sodium acetate, pH 5 in the (A) absence of NaCl and (B) in the presence of NaCl. Concentration of nanometer sized protein particles formed due to each stress at day 1 (D1) and (D3) in the presence and absence of NaCl (C, D). Each data point are the average of three separate experiments (n=3) and the error bars for each data point represent the 95% confidence interval.

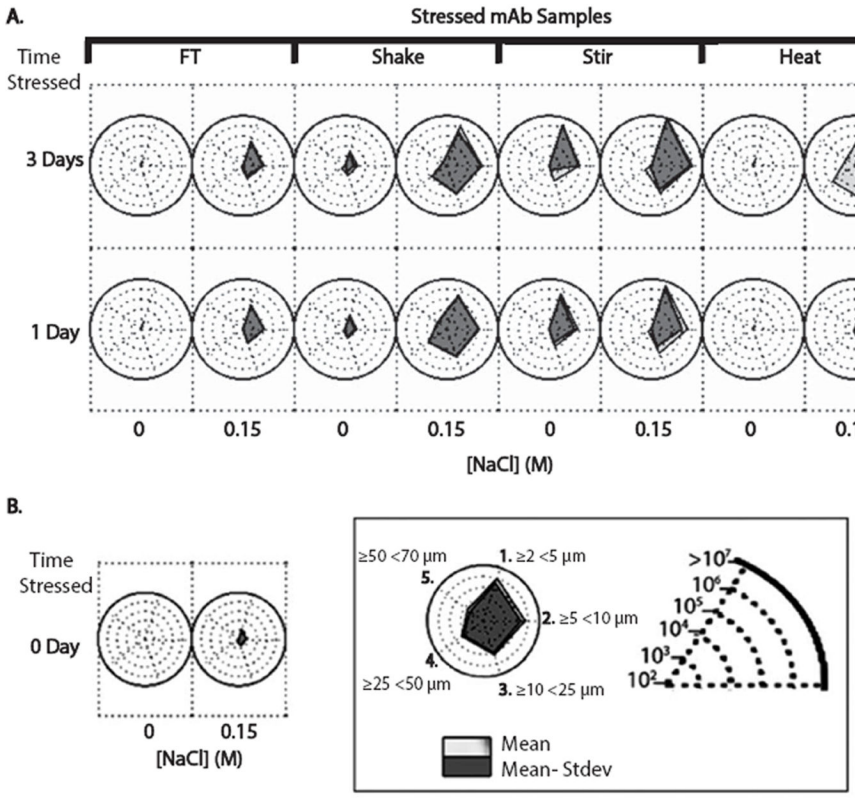


**Figure 3.**

Radar plots for visualizing formation of subvisible particles (concentration and size distributions) in IgG1 mAb solutions exposed to different stresses as measured by MFI. Radar plots show MFI particle concentration and size data distributions as generated by four indicated stresses when applied to 1 mg/mL antibody solution containing 10 mM sodium acetate, pH 5 with and without 150 mM NaCl. See text for details of radar plot analysis. The data shown are the average of three separate experiments (n=3) and the error represents the 95% confidence interval.

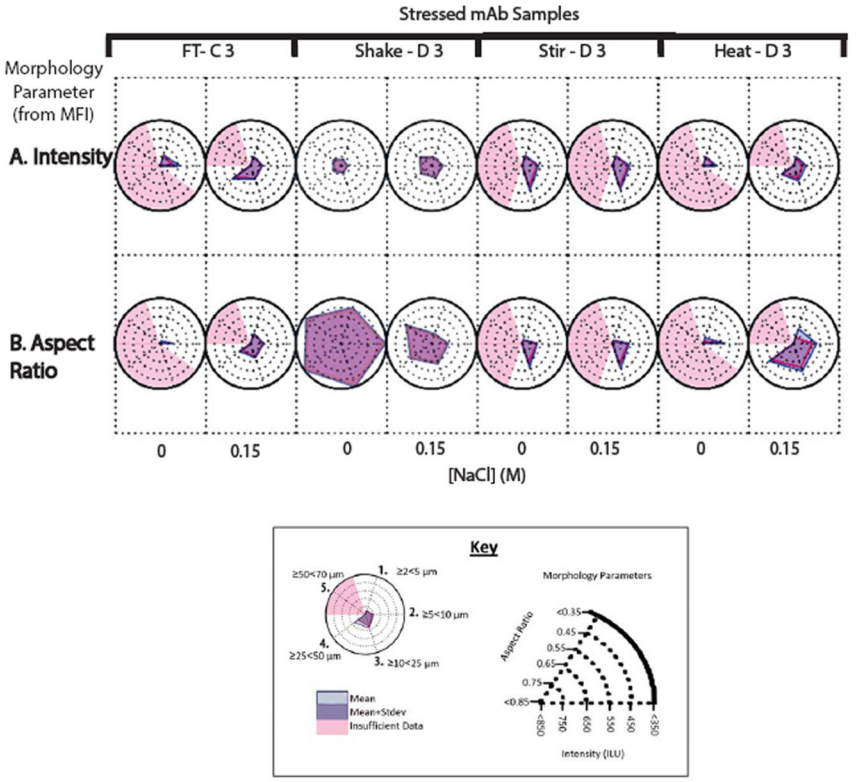


**Figure 4.**

Radar plots for visualizing morphology parameters of subvisible particles (aspect ratio and intensity) in IgG1 mAb solutions exposed to different stresses as measured by MFI. Radar plots show MFI morphology data distributions as generated by four indicated stresses when applied to 1 mg/mL antibody solution containing 10 mM sodium acetate, pH 5 with and without 150 mM NaCl. See text for details of radar plot analysis. The data shown are the average of three separate experiments (n=3) and the error represents the 95% confidence interval.

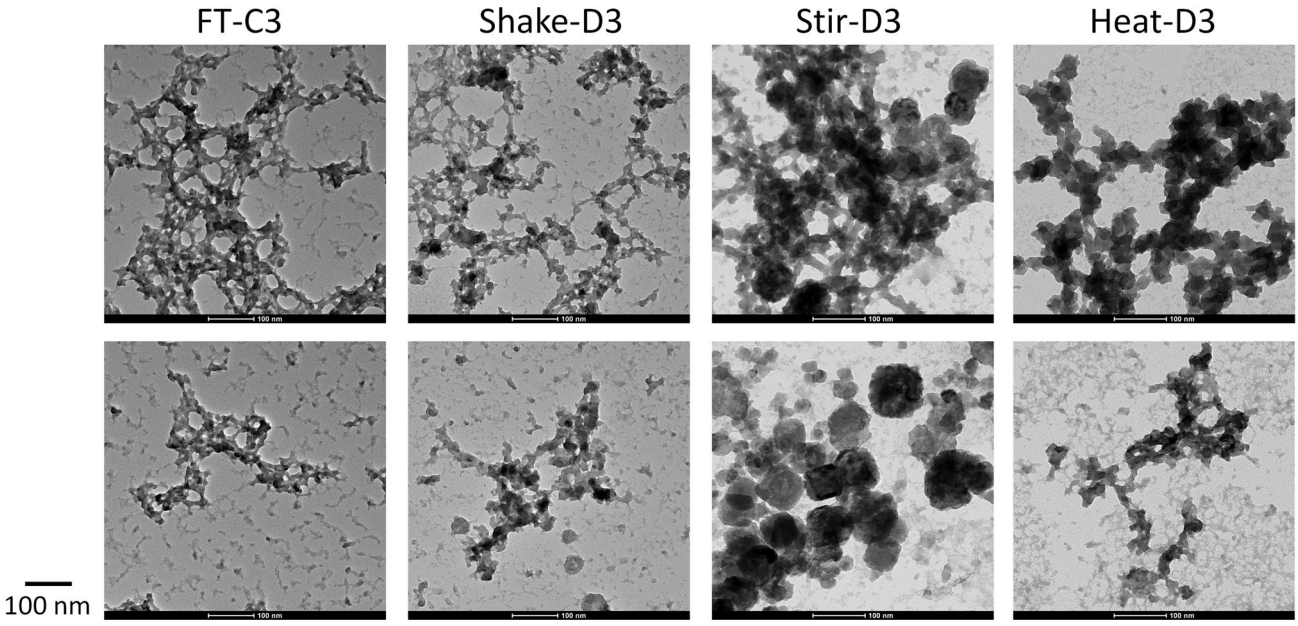


**Figure 5.**

Representative TEM images of IgG1 mAb aggregates and particles formed after 3 freeze-thaw cycles or three days of each indicated stress. Particles were isolated from 1 mg/mL antibody solution in 10 mM sodium acetate, 150 mM NaCl, pH 5.

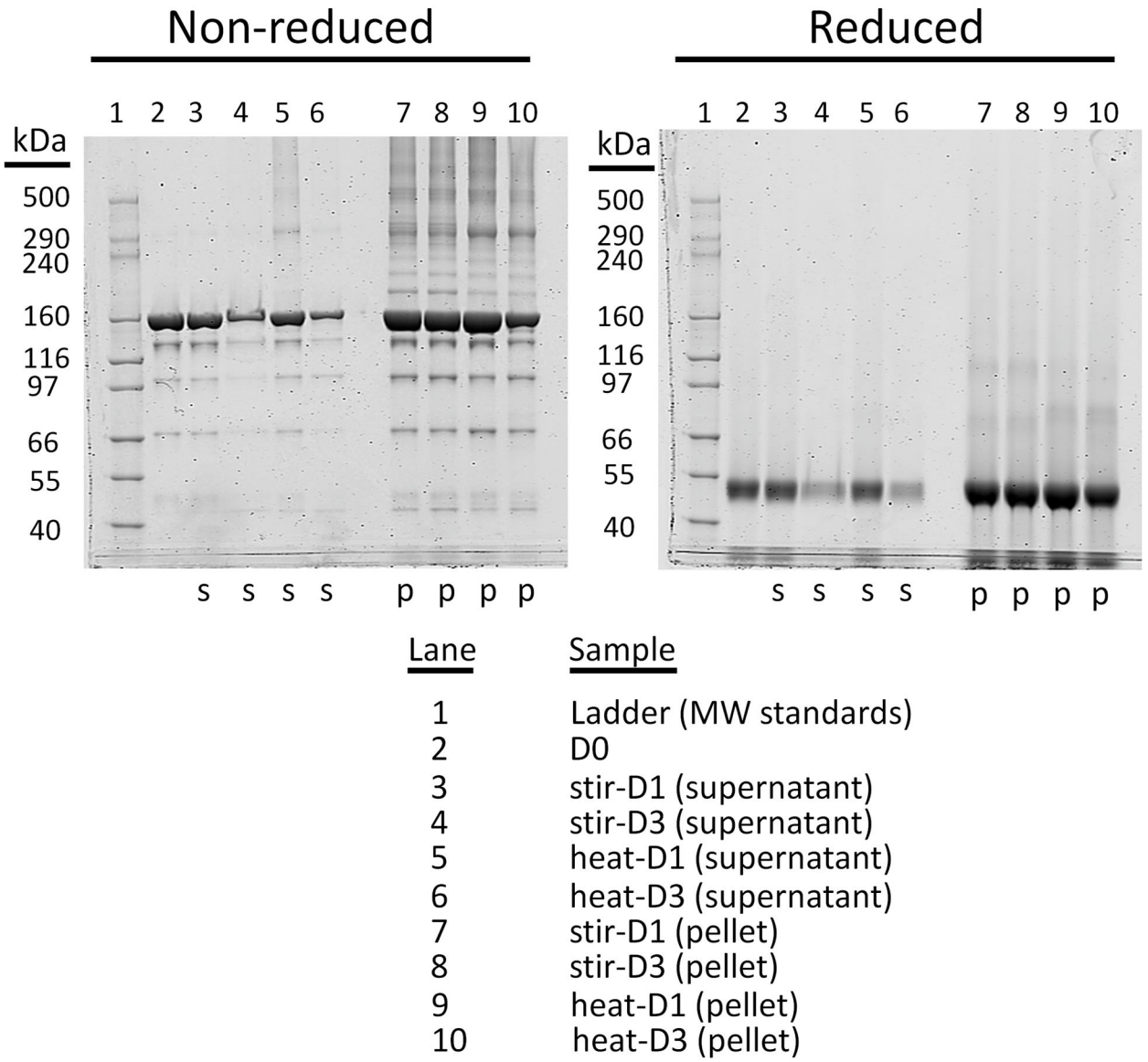


**Figure 6.**

Reduced and non-reduced SDS-PAGE gels of IgG1 mAb samples exposed to four different stresses. Samples contained 1 mg/ml antibody in 10 mM sodium acetate, 150 mM NaCl, pH 5. High molecular weight aggregates formed by disulfide linkages were observed in pellet of stir-Day 1, stir-Day 3, heat-Day 1 and heat-Day 3 samples. Stressed samples were centrifuged to separate supernatant (S) from pellet (P), run on SDS-PAGE, and stained as described in methods section.

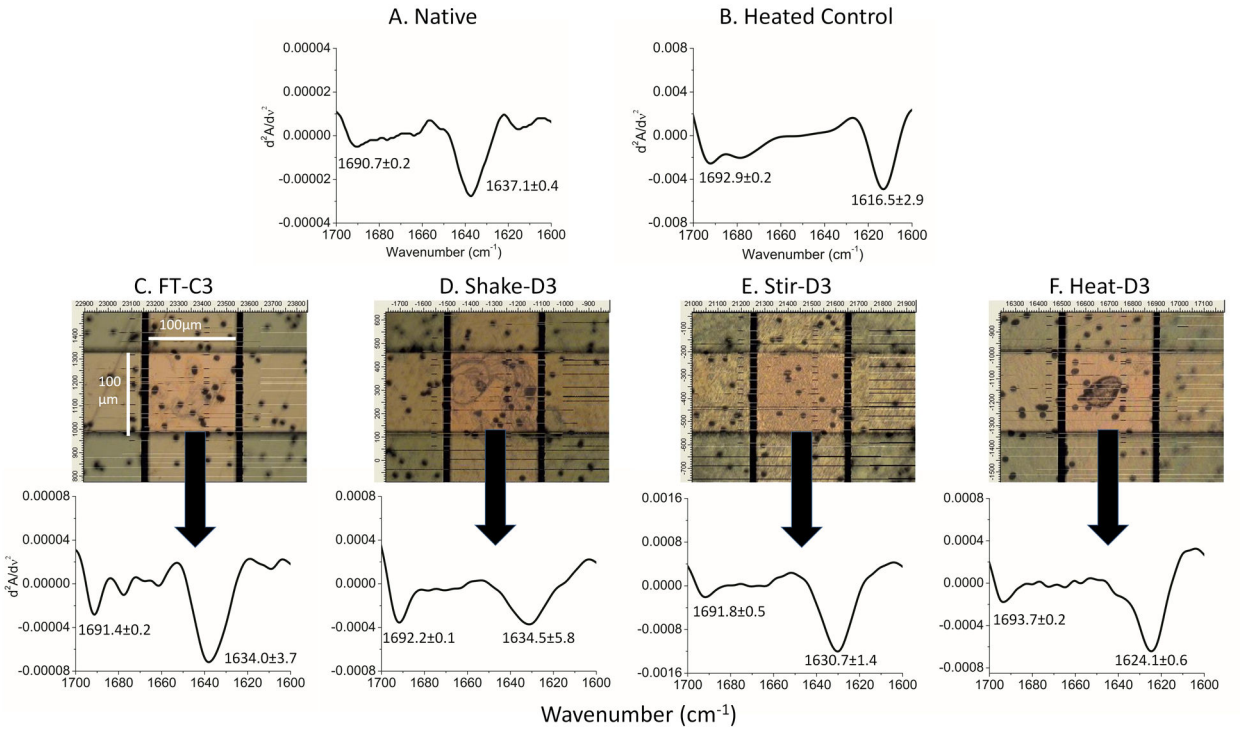


**Figure 7.**

FTIR analysis of overall secondary structure of IgG mAb solutions and isolated particles as generated from four indicated stresses. Samples contained 1 mg/ml antibody in 10 mM sodium acetate, 150 mM NaCl, pH 5. Second derivative FTIR spectrum of (A) native, unstressed protein in solution, and (B) mAb heated at 80°C for 20 min to determine the maximum extent of secondary structure loss in solution, (C, D, E, F) Representative optical images of isolated mAb particles (by passing through gold filter) as generated from the four indicated stresses and their corresponding second derivative FTIR spectra from FTIR microscope. Numerical values are the average of three separate experiments (n=3) with error associated with the wavenumbers representing the 95% confidence interval.

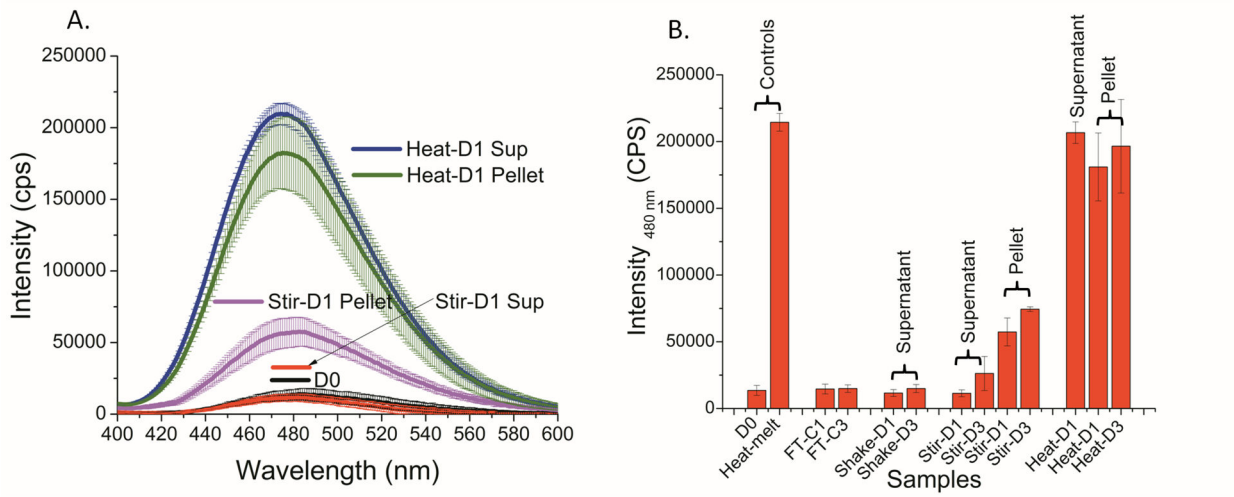


**Figure 8.**

ANS extrinsic fluorescence analysis of IgG1 mAb samples (supernatant and pellet components) before and after indicated stress was applied to samples. Samples contained 1 mg/ml mAb in 10 mM sodium acetate, 150 mM NaCl, pH 5. (A) Representative ANS spectra, and (B) ANS fluorescence intensity values (at 480 nm) for each stressed mAb sample compared to the two controls: unstressed (D0) and extensively heated samples (Heat-melt). The average intensities shown are based on three separate experiments (n=3). The error bars represent 95% confidence interval.

**Table 1**

Turbidity measurements and visual assessments of visible particles were performed on control and stressed mAb samples. Samples contained 1 mg/mL antibody in 10 mM sodium acetate, pH 5 in absence and presence of 150 mM NaCl. The turbidity data are an average of three independent experiments (n=3) with standard deviation. For visual assessments of visible particles, "-" is no change observed relative to unstressed sample; "+" some change observed relative to unstressed sample (2-5 particles detected); "++" notable change observed relative to unstressed sample (> 5 particles detected).

| | **Turbidity (NTU)** | | **Visual Assessment** | **Turbidity (NTU)** | | **Visual Assessment** |
|---|---|---|---|---|---|---|
| | **No NaCl** | | | **With 150 mM NaCl** | | |
| **mAb Samples** | ***Average*** | ***Stdev*** | | ***Average*** | ***Stdev*** | |
| Buffer Alone (no mAb) | 0.2 | 0.1 | - | 0.7 | 0.6 | - |
| Day 0 | 0.6 | 0.1 | - | 0.7 | 0.1 | - |
| Freeze-Thaw Cycle 1 | 1.3 | 0.3 | - | 0.7 | 0.1 | - |
| Freeze-Thaw Cycle 3 | 1.5 | 0.5 | - | 1.6 | 0.2 | - |
| Agitation Day 1 | 8.1 | 1.6 | ++ | 22.4 | 2.1 | ++ |
| Agitation Day 3 | 7.6 | 0.4 | ++ | 25 | 10.5 | ++ |
| Stirring Day1 | 13.2 | 5.4 | ++ | 217.7 | 17 | ++ |
| Stirring Day3 | 64.4 | 7 | ++ | 756.7 | 71.9 | ++ |
| Heating Day1 | 0.9 | 0.1 | - | 82.4 | 3.4 | + |
| Heating Day3 | 0.9 | 0.1 | - | 212.3 | 5.9 | ++ |

**Table 2**

Summary of formation of soluble aggregates and nanometer, subvisible (microns), and visible (>100μm) sized particles as measured by SEC, NTA, MFI, Turbidity, and Visual Assessments, respectively. Symbols describe whether a change was observed (+) or not observed (-) compared to the unstressed mAb sample with the given analytical technique. Eight types of measurements are shown in the table and the last column summarizes, for each stress, the number of notable effects (+ vs. -) due to the presence vs. absence of NaCl observed for each assay. Samples contained 1 mg/mL antibody in 10 mM sodium acetate, pH 5 in absence and presence of 150 mM NaCl.

| | SEC[a] | | | | NTA | MFI | Turbidity | Visual Assessment | # Results differed (±NaCl) |
|---|---|---|---|---|---|---|---|---|---|
| | %M | %I | %A | %F | | | | | |
| **Freeze/Thaw** | | | | | | | | | |
| -NaCl | - | - | - | - | - | - | - | - | |
| +NaCl | - | + | - | - | + | + | - | - | **3/8** |
| **Agitation** | | | | | | | | | |
| -NaCl | - | - | - | - | - | + | + | + | |
| +NaCl | - | + | - | - | - | + | + | + | **1/8** |
| **Stirring** | | | | | | | | | |
| -NaCl | - | + | - | - | + | + | + | + | |
| +NaCl | + | + | - | - | + | + | + | + | **1/8** |
| **Heating** | | | | | | | | | |
| -NaCl | - | + | - | + | - | + | - | - | |
| +NaCl | + | + | + | - | + | + | + | + | **6/8** |

[a] %M, %I, %A, %F correspond to percent monomer, insoluble aggregate, soluble aggregate, and fragment, respectively.